Control Allocation with Dynamic Weight Scheduling for Two-task Integrated Vehicle Control

Barys Shyrokau and Danwei Wang
EXQUISITUS, Centre for E-City, Nanyang Technological University

50 Nanyang Avenue, S2-B6-01, 639798, SINGAPORE
Phone: +65 6790-4053
Fax: +65 6793-3318
E-mail: barys1@e.ntu.edu.sg

This paper describes a multi-layer structure based on control allocation with dynamic weight scheduling. The computational investigation of the proposed control structure is carried out using 14 DoF vehicle model in the wide range of vehicle curvilinear motion for 'Sine with Dwell' test. The proposed control allocation with dynamic weight scheduling demonstrates lower energy loss without significant impairment of stability of motion and vehicle handling compared to control allocation with fixed weight distribution.

Topics / Integrated Chassis Control

1. INTRODUCTION

Modern concepts of electric passenger vehicles have distributed electric drives, active brakes, steering and suspension. Moreover, the application of active autonomous wheels, such as Michelin Active Wheel, Siemens E-Corner, when automotive subsystems are placed into the wheel, has been started. It can be argued, a near future vehicle will be an over-actuated system. This feature allows the implementation of a stand-alone/joint actuation of active subsystems for vehicle control.

The different ways to change force components in the tyre-road contact, are shown in the Fig. 1 (based on [1] and extended). The available control inputs are eight per wheel (in the case of individual subsystems for each wheel) plus additional inputs related to aerodynamics and anti-roll bars. Moreover, specific automotive systems have no wide application or they are being developed, like control of contact tyre temperature; and the final number of control inputs is increased. This tendency increases the feasibility and potential of integrated control. In this paper, only three subsystems, such as active brake/drive system and front steering, are considered.

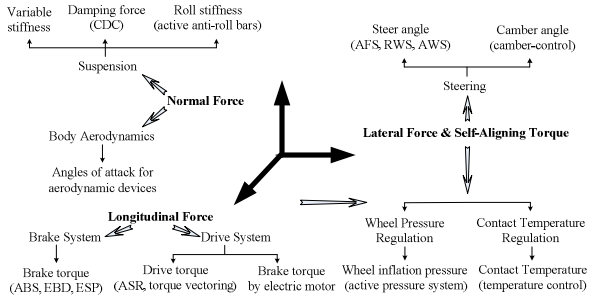

Fig. 1 Ways to change tyre forces

The basic function of integrated chassis control is active safety; however, reduction of fuel/energy consumption and energy loss became significant over last years. As a result, the minimum of energy consumption and energy loss is a key performance indicator for modern vehicle control.

An intuitive solution to reach active safety and energy consumption is to combine tracking and energy problems into one integrated control solution. However, the priority of two tasks, most likely, depends on driving conditions. For instance, friction brakes can ensure fast correction of vehicle motion, but the result of actuation is a loss of velocity. When the time of correction is not so critical, the priority of energy consumption can be higher than in the first case. The correction of motion can be obtained by the combination of steering and drive actuations.

Moreover, there are many additional specific requirements, such as vehicle handling, ride comfort, traction/braking performance, tyre aging and others.

Hence, the modern control of vehicle motion should solve various control tasks, and some of them are contradictory in nature.

This paper describes the investigation of control structure for integrated vehicle control, based on the control allocation with dynamic weight scheduling, to reach multi-task control, specifically, to reduce energy loss without significant impairment of stability of motion and vehicle handling.

2. VEHICLE MODEL

The vehicle model describes the behavior of the vehicle body in the space and the vertical and rotational motion of each wheel. Hence, it has 14 DoF, which allows us to receive more realistic vehicle behavior. The

steering system includes a kinematic model and dynamic effects associated with roll and compliance steer. The model of the electric driveline includes Thevenin battery model and four electric motors, which are represented by look-up tables with data from a real in-wheel motor. The transient processes in the electric motors are described by first-order plus time delay transfer function. The brake system is electro-hydraulic and it consists of a tandem master cylinder with a spring pedal travel simulator, a brake fluid reservoir, a hydraulic pump with a pump motor, a high-pressure hydraulic accumulator, block valves, compensating valves, control inlet/outlet valves for pressure build-up and decrease at each wheel, and brake mechanisms. To characterize the steady-state tyre behavior, the Pacejka tyre model is used. For transient tyre behavior, a relaxation length model is added. The developed vehicle model is realized in Matlab/Simulink. The mathematical description of developed model and its verification with multibody model from commercial software IPG/Maker is described in the paper [2] due to publication limits.

3. CONTROL STRUCTURE

The proposed control structure has a multi-layer architecture. It is shown in Figure 2.

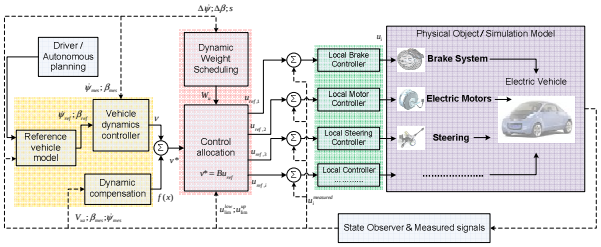

Fig. 2 Control Structure

There are three layers in the control structure. The upper layer (yellow) defines reference behavior of vehicle, a required virtual control effort (total lateral force and yaw torque) to minimize difference between reference and actual behavior, and correction of the virtual control effort based on feedback linearization. The middle layer (pale red) is applied for control allocation and it includes two blocks. The first block is related to weighted optimal control allocation for an over-actuated system. The second block defines the priority of each subsystem according to assessment criteria, which are discussed below. The lower layer of the control structure (green) is a layer comprising the local controller of each subsystem. Moreover, the boundary conditions for optimization are defined in this layer.

3.1 Upper Layer

The model-following approach is used for vehicle dynamics control. The linearized vehicle model is shown in Appendix. The selected vehicle states are the yaw rate and vehicle sideslip angle. The yaw rate and lateral acceleration can be measured by standard onboard sensors. The measurement of the sideslip angle is very difficult, and usually it is estimated. It is assumed that the yaw rate and sideslip angle are always available and the measurement noise is ignored.

To describe the planar motion, the 2 DoF bicycle vehicle model is used as a reference model. The motion dynamics can be presented as follows [3]:

$$\begin{bmatrix}\dot{\beta}\\ \ddot{\psi}\end{bmatrix}=\begin{bmatrix}-\frac{C_f+C_r}{m_aV_{xa}} & -1+\frac{-aC_f+bC_r}{m_aV_{xa}^2}\\ \frac{-aC_f+bC_r}{I_{zz}} & -\frac{a^2C_f+b^2C_r}{I_{zz}V_{xa}}\end{bmatrix}\begin{bmatrix}\beta\\ \dot{\psi}\end{bmatrix}+\begin{bmatrix}\frac{C_f}{m_aV_{xa}}\\ \frac{aC_f}{I_{zz}}\end{bmatrix}\delta_f \quad (1)$$

The reference yaw rate and vehicle sideslip angle are calculated as [4]:

$$\dot{\psi}^{ref}=\begin{cases}\dot{\psi}, & |\dot{\psi}|\le|\dot{\psi}_{\max}|\\ \pm\dot{\psi}_{\max}, & \text{otherwise}\end{cases} \quad (2)$$

$$\beta^{ref}=\begin{cases}\beta, & |\beta|\le|\beta_{\max}|\\ \pm\beta_{\max}, & \text{otherwise}\end{cases} \quad (3)$$

The maximum of the reference yaw rate, obtained beyond the adhesion tyre limit, should be limited [5]:

$$\dot{\psi}_{\max}=0.85\frac{\mu g}{V_{xa}} \quad (4)$$

The maximum of the vehicle sideslip angle is [4]:

$$\beta_{\max}=\frac{\pi}{180}\begin{cases}10^0-7^0\frac{V_{xa}^2}{40^2}, & V_{xa}<40\\ 3^0, & V_{xa}\ge 40\end{cases} \quad (5)$$

The control errors are calculated as:

$$e_\beta=\begin{cases}\beta_{ref}-\beta_{mes}, & |\beta_{ref}-\beta_{mes}|>\Delta_\beta\\ 0, & |\beta_{ref}-\beta_{mes}|<\Delta_\beta\end{cases} \quad (6)$$

$$e_{\dot{\psi}}=\begin{cases}\dot{\psi}_{ref}-\dot{\psi}_{mes}, & |\dot{\psi}_{ref}-\dot{\psi}_{mes}|>\Delta_{\dot{\psi}}\\ 0, & |\dot{\psi}_{ref}-\dot{\psi}_{mes}|<\Delta_{\dot{\psi}}\end{cases} \quad (7)$$

The different control strategies can be applied to calculate virtual control effort. In this paper, the PI control is applied. The cancelation of nonlinear component *f(x)* is used for feedback linearization [6]:

$$\nu=-f(x)+K_pe+K_i\int edt \quad (8)$$

3.2 Middle Layer

Control allocation

The control allocation (CA) technique has a wide application in the area of vehicle motion control. In accordance with [7] control allocation can be divided into static and dynamic. In static CA, the actuators have immediate effect on the virtual control inputs. Dynamic CA assumes that each actuator has its own dynamics, which can differ from the others. Depending on parameters included in the input control matrix, the CA can be 'direct' or 'indirect' CA [8]. The first type is defined by actuator parameters. The second uses intermediate parameters in the control input. The parameters can be:

- longitudinal and lateral tyre forces [8, 9];
- kinematic parameters of the tyre (longitudinal slip and wheel slip angles) [10, 11];
- actuator inputs (brake and drive torques, steering angle) [12-15];
- mixed output, for instance, longitudinal forces and steering angle [6].

The control allocation methods include

pseudo-inverse, direct, daisy-chain, and optimization-based CA. These methods are well described theoretically in [7].

In the general case, the relation between virtual and reference controls is nonlinear. Using the linearized vehicle model from Appendix and feedback linearization, the weighted l_2-optimal control allocation problem can be formulated as to minimize an allocation error and actuations, taking into account actuator constraints. This problem can be solved in one step using weighted least squares [12]:

$$u_{ref} = \arg \min_{\underline{u}_{ref} \le u_{ref} \le \overline{u}_{ref}} \left(\left\| W_u (u_{ref} - u_{des}) \right\|_2^2 + \xi \left\| W_v (B u_{ref} - v) \right\|_2^2 \right) \quad (9)$$

The fixed-point method is suitable for the application in the real-time systems to solve optimization problem [10].

Since CA regulates a nonlinear object like an electric vehicle, and the parameters of vehicle motion vary in the wide range, certain adaptation techniques can be used:

- update law for control effectiveness matrix B [16];
- update laws for input control parameters [17].

From another side, as we noted in the Introduction, the modern control should be multi-task. For this purpose, the more complex cost function can be used extended by components related to control tasks. For instance, Chen and Wang [14] added power consumption (related to power consumption of all in-wheel motors in different modes) into the cost function, and called the method as “energy-efficient control allocation”. Kang et al. [15] included in the cost function not only energy efficiency, but also energy loss (slip control).

However, there is a technique, which allows multitasking without increasing of cost function complexity. Laine and Fredrikson [12] noted that subsystems penalization can be provided by the scheduling of weighting matrix W_u. Later Tagesson and colleagues [18] used a weighting matrix to prioritize brake pressures according to normal force distribution during heavy vehicle braking to obtain better vehicle stability. However, the issues of dynamic scheduling for multi-task integrated control with more number of vehicle subsystems as well as the control laws for the weight scheduling of such variant are not considered.

Hence, the research aim is to develop a dynamic prioritization of more than two vehicle subsystems, taking into account the tasks of vehicle motion control.

Concept of dynamic weight scheduling

The idea is to prioritize each vehicle subsystem in accordance with some assessment criteria, which is related to vehicle operational properties. On the left-hand graph of Fig. 3 the typical variant of the system priority for control allocation is shown. All subsystems have the same priority and participate in the regulation process with equal weights. On the right-hand graph of Fig. 3 the instance for control error of yaw rate is shown. If the control error of yaw rate is small, the compensation can be realized by the steering and drive system. It allows to reduce the usage of the brake system to decrease non-recuperative energy losses. When the level of control error is increased, the participation of the brake system becomes more important.

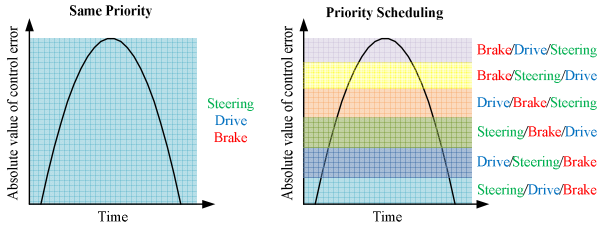

Fig. 3 Example of dynamic weight scheduling

The following arguments for the application of unequal weights can be provided:

- dynamics of each actuator is unique, and, as a consequence, the rate of influence on vehicle behavior is different. As a result, the transient process can be slower or faster;
- each type of actuator has own internal energy consumption and energy efficiency;
- load levels acting on vehicle during subsystem actuation are different, for instance, longitudinal and lateral rolling resistance;
- some actuators can be used not only as motors, but also as generators. They have a function of energy recuperation.

Moreover, in [19] the authors showed that the different contribution of each subsystem to the regulation process defines tracking accuracy and energy consumption. Therefore, the priority of each subsystem should be changed during vehicle control.

Proposed dynamic weight scheduling

The proposed weight scheduling for multi-task control includes the following stages:

(1) Selection of the assessment criteria to characterize each task of vehicle dynamics control. In this paper, the error of yaw rate defines vehicle handling and stability, the error of sideslip angle is used for vehicle stability. The average longitudinal slip is associated with energy loss.

(2) Choice of vehicle subsystems which will be involved in the regulation process. In this paper, there are steering, drive and brake systems.

(3) Definition of the weight functions regarding each assessment criterion and each subsystem. Examples of weight functions for the error of yaw rate are shown in Fig. 4. The influence of stand-alone vehicle subsystems on vehicle dynamics is well presented in [20]. These weight functions are set-up on the design stage. *The lower weight means higher priority.*

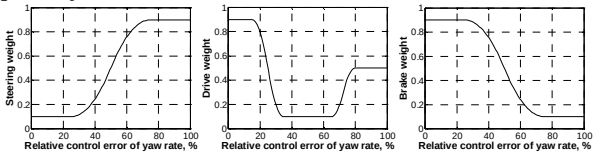

Fig. 4 Weight functions for the error of yaw rate

(4) The weight of each subsystem is calculated as the algebraic sum of weight functions for all assessment criteria:

$$W^*_{steer} = \gamma_1 f^{steer}_{\psi}\left(|e_{\psi}|\right) + \gamma_2 f^{steer}_{\beta}\left(|e_{\beta}|\right)$$
$$W^*_{drive} = \gamma_1 f^{drive}_{\psi}\left(|e_{\psi}|\right) + \gamma_2 f^{drive}_{\beta}\left(|e_{\beta}|\right) + \gamma_3 f^{drive}_{slip}\left(|\bar{s}_w|\right) \quad (10)$$
$$W^*_{brake} = \gamma_1 f^{brake}_{\psi}\left(|e_{\psi}|\right) + \gamma_2 f^{brake}_{\beta}\left(|e_{\beta}|\right) + \gamma_3 f^{brake}_{slip}\left(|\bar{s}_w|\right)$$

The parameters γ_i define the priority of each assessment criterion. In this publication, γ_1=0.1, γ_2=0.4, γ_3=0.5. Finally, all weights are assumed to be normalized, i.e. their sum equals one:

$$W_{steer} = \frac{W^*_{steer}}{\sum_{i=1}^{3} W_i} \qquad W_{drive} = \frac{W^*_{drive}}{\sum_{i=1}^{3} W_i} \qquad W_{brake} = \frac{W^*_{brake}}{\sum_{i=1}^{3} W_i} \quad (11)$$

The proposed approach allows us to prioritize each subsystem during regulation. Moreover, control tasks related to vehicle stability, vehicle handling or energy loss can be prioritized by parameters γ_i as well. The difference between application of matrix W_v and parameters γ_i is that all control tasks remain their priority in the optimization problem to minimize an allocation error. The prioritization of control tasks is carried out in the framework of subsystem actuations.

3.3 Bottom Layer

The aim of local controllers is to compensate for the difference between reference control signals obtained from the middle level and actual signals obtained by direct measurement or by online estimation. The second aim of local controllers is to provide boundary conditions for control allocation taking into account actuator limits and wheel slip control.

Active front steering controller

The reference control input for the steering system is calculated as the sum of the angles obtained from driver input and from control allocation. Since a kinematic model represents the steering system, the actual steering input is equal to reference control input.

In-wheel motor controller

The in-wheel motor controller is a PI controller. It is assumed, estimated real torque is obtained from the estimation procedure.

$$u_i^{drive} = K_p^{drive}\left(M_i^{em,ref} - \hat{M}_i^{em,act}\right) + K_i^{drive}\int\left(M_i^{em,ref} - \hat{M}_i^{em,act}\right)dt \quad (12)$$

The torque limit of an electric motor can be found as [21]:

$$M_i^{em,\lim} = M_i^{em,\max}\prod w_i\left(T_i, SOC, V_{xa}, U_i, fault\right) \quad (13)$$

The maximum overload torque of an electric motor is obtained from the look-up table of the torque map of the electric motor, which is placed into the controller. The torque limit is corrected by weighed coefficients, which are related to electric motor temperature, state-of-the-charge, longitudinal vehicle velocity, under and overvoltage protection and fault control. Selection of these weighted coefficients is shown detailed in [2].

Brake system controller

Under normal working conditions, the PID control of the inlet and outlet valves is applied to realize the pressure tracking control. The error is calculated as a difference between measured and reference pressure for each wheel. The reference brake pressure is found as:

$$p_i^{reference} = \frac{M_i^{br,ref}}{\mu_0 S_{cyl} r_e} \quad (14)$$

The control law for the pressure controller is:

$$u_i^{brake} = K_p^{brake} e_i + K_i^{brake}\int e_i dt + K_d^{brake}\frac{de_i}{dt} \quad (15)$$

The constructive parameters of brake mechanism and the level of wheel slip restrict the torque limit of friction brake. The correction taking into account wheel slip is carried out based on the threshold of wheel slip. The algorithm is rule-based and similar to control of anti-lock brake system [22].

4. Simulation Results and Discussion

The maneuver simulated is 'Sine with Dwell' at initial velocity of 80 km/h and max. steering amplitude of 140 deg on the dry asphalt. Three variants are considered: (1) uncontrolled motion, (2) controlled motion based on proposed control structure with fixed weight distribution between vehicle subsystems, and (3) controlled motion with dynamic weight scheduling. The simulation results of vehicle motion are shown in Fig. 5.

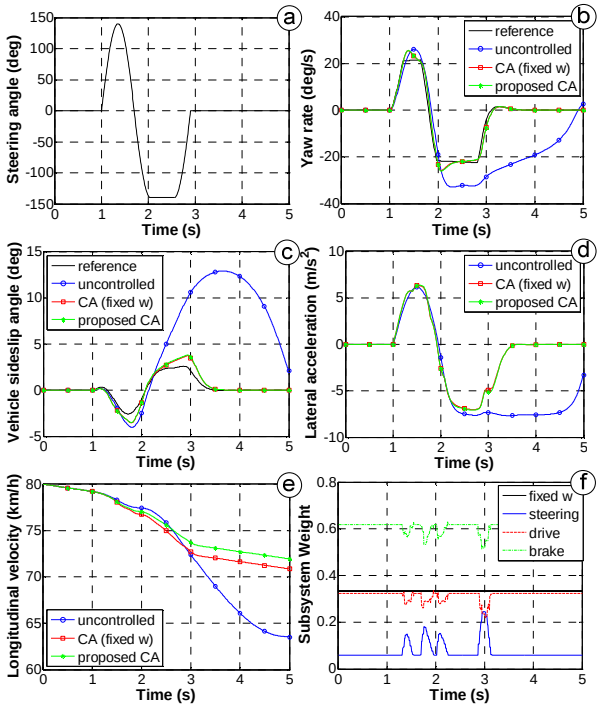

Fig. 5 Simulation results of vehicle motion

The input steering law is depicted in Fig. 5a. For uncontrolled vehicle, the yaw rate (Fig. 5b) and sideslip angle (Fig. 5c) are increased, and the uncontrolled vehicle slips on the lateral direction as shown in Fig. 5d. The controlled vehicle moves closer to reference vehicle model. The difference between CAs with fixed and dynamic weights for yaw rate and sideslip angle is insignificant. Therefore, both controllers insure high handling and stability (Fig. 5b-d).

Meanwhile, the difference of velocities between CAs with fixed and dynamic weights at the end of maneuver (Fig. 5e) is up to 1.1 km/h. The velocity loss of proposed CA in the percentage level is less of 1.5%

compared to CA with fixed weights. The weight change during maneuver is shown in Fig. 5f. For CA with fixed weights each subsystem has the same weight. It should be noted, the reduction of velocity loss is mainly defined by initial prioritization of each subsystem (different initial weights). The weight changing during motion is directed to improve tracking accuracy under higher control errors.

The subsystem actuations for both CAs are shown in Fig. 6. The left-hand graphs are related to CA with fixed weights, and right-hand ones to proposed CA. The application of friction brake is up to two times less for proposed CA. This fact allows us to argue, the internal energy consumption of brake system will be lower in proposed CA.

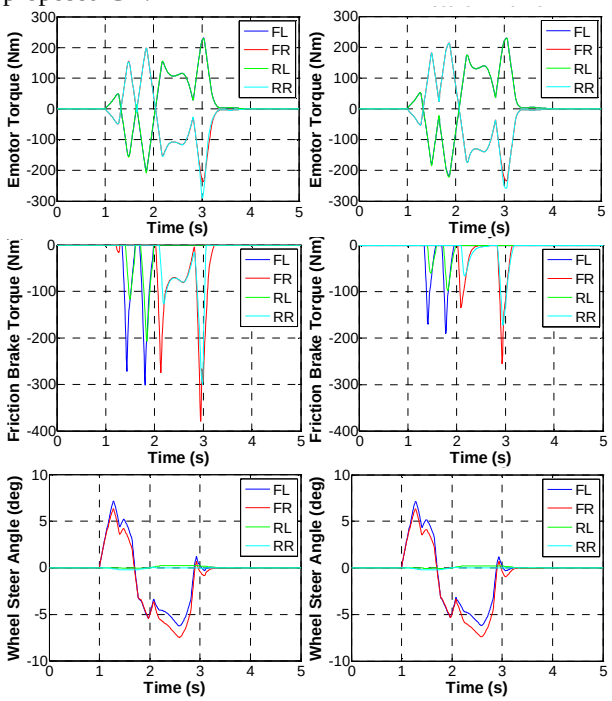

Fig. 6 Actuations during 'Sine with Dwell' test:
FL – front left; FR – front right; RL – rear left; RR – rear right

To evaluate the functionality and effectiveness of the proposed control structure in the wide range of vehicle motion, the simulation is carried out with variation of initial parameters of 'Sine with Dwell' test, such as initial velocity and maximum amplitude of steering angle. To assess vehicle dynamics, the RMS error of yaw rate and sideslip angle are calculated as:

$$\sigma_{(\dot{\psi} \text{ or } \beta)} = \sqrt{\frac{1}{n}\sum_{i=1}^{n}\left((\dot{\psi} \text{ or } \beta)_{ref} - (\dot{\psi} \text{ or } \beta)_{mes}\right)^2} \quad (16)$$

Another important indicator is a loss of longitudinal velocity during maneuver, which is founded in the percentage level:

$$\Delta V_{xa}^{loss} = 100\frac{V_{xa}^{init} - V_{xa}}{V_{xa}^{init}} \quad (17)$$

Simulation results of the effectiveness of proposed control structure at different initial longitudinal velocity and max. steering angle is shown in Fig. 7. The left-hand graphs are related to CA with fixed weights, and right-hand ones to proposed CA. The RMSE's of yaw rate and sideslip angle are close in value for the wide range of motion. Meanwhile, the proposed dynamic weight scheduling always shows higher velocity at the end of maneuver compared to CA with fixed weights.

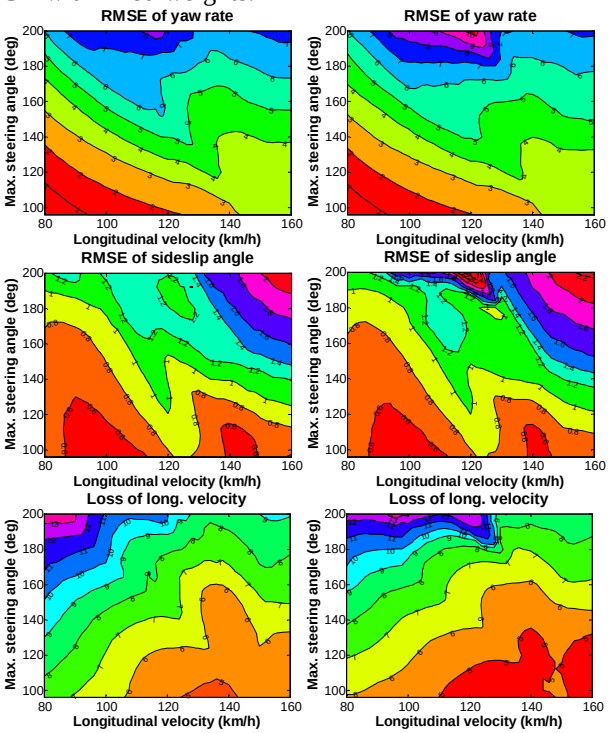

Fig. 7 Effectiveness of proposed control structure

5. CONCLUSION

This paper describes a multi-layer control structure based on control allocation with dynamic weight scheduling. The upper level defines vehicle motion control, which is based on PI control and feedback linearization using nonlinear component of linearized model of vehicle motion. The middle layer of control allocation is considered as weighted l_2-optimal control allocation. The control allocation is optimization-based and solved by fixed-point method. The dynamic weight scheduling for vehicle subsystems was introduced into the control allocation. The proposed control allocation with dynamic weight scheduling allows us to prioritize vehicle subsystems during motion. The lower layer shows local controllers for steering, drive and brake subsystems. They compensate a difference between the reference and the actual signals obtained. Moreover, the boundary limits for control allocation are calculated by taking into account actuator physical limits and wheel slip control.

The computational investigation of the developed control structure was carried out using 14 DoF vehicle model in the wide range of vehicle motion for 'Sine with Dwell' test (longitudinal velocity from 80 km/h to 160 km/h, and max. wheel steering angle from 100 deg to 200 deg). The proposed control allocation with dynamic weight scheduling demonstrates lower energy loss without significant impairment of stability of motion and vehicle handling compared to control allocation with fixed weight distribution.

ACKNOWLEDGMENTS

This publication is made possible by the Singapore National Research Foundation under its Campus for Research Excellence And Technological Enterprise (CREATE) programme. The views expressed herein are solely the responsibility of the authors and do not necessarily represent the official views of the Foundation.

REFERENCES

[1] Li, D. et al. "A top-down integration approach to vehicle stability control", Proc. of IEEE Conference on Vehicular Electronics and Safety, 2007, pp. 1-6.
[2] Shyrokau, B. et al. "Vehicle Dynamics Control with Energy Recuperation based on Control Allocation for Independent Wheel Motors and Brake System", Int. Journal of Powertrains, 2012 (submitted)
[3] Chen, B.C., Hsieh, F.C. "Sideslip angle estimation using extended Kalman filter", Vehicle System Dynamics, 2008, vol. 46, pp. 353-364
[4] Kiencke, U., Nielsen, L. "Automotive control systems: for engine, driveline, and vehicle", Springer, 2005
[5] Rajamani, R. "Vehicle dynamics and control", Springer, 2006
[6] Hac, A. et al. "Unified Control of Brake- and Steer-by-Wire Systems Using Optimal Control Allocation Methods", SAE Technical Paper, 2006, 2006-01-0924
[7] Härkegård, O. "Backstepping and control allocation with applications to flight control", PhD thesis, Linköpings universitet, 2003
[8] Gerard, M., Verhaegen, M. "Global and local chassis control based on Load Sensing", Proc. of American Control Conference, 2009, pp. 677-682
[9] Schofield, B., Hagglund, T. "Optimal control allocation in vehicle dynamics control for rollover mitigation", Proc. of American Control Conference, 2008, pp. 3231-3236
[10] Wang, J. "Coordinated and reconfigurable vehicle dynamics control", PhD thesis, University of Texas Libraries, Austin, 2007
[11] Bayar, K. et al. "Development of a vehicle stability control strategy for a hybrid electric vehicle equipped with axle motors", Proc. of IMechE Part D: J. Automobile Engineering, 2012.
[12] Laine, L., Fredriksson, J. "Coordination of Vehicle Motion and Energy Management Control Systems for Wheel Motor Driven Vehicles", Proc. of Intelligent Vehicles Symposium, 2007, pp. 773-780.
[13] Plumlee, J. H. et al. "Control of a ground vehicle using quadratic programming based control allocation techniques", Proc. of American Control Conference, 2004, vol.5, pp. 4704-4709.
[14] Chen, Y., Wang, J. "Energy-efficient control allocation with applications on planar motion control of electric ground vehicles", Proc. of American Control Conference, 2011, pp. 719-724.
[15] Kang, J. et al. "Control Allocation based Optimal Torque Vectoring for 4WD Electric Vehicle", SAE Technical Paper, 2012, 2012-01-0246
[16] Lu, X., Zhuoping, Y. "Control allocation of vehicle dynamics control for a 4 in-wheel-motored EV", Proc. of Conference on Power Electronics and Intelligent Transportation System, 2009, pp. 307-311.
[17] Tjonnas, J., Johansen, T. A. "Stabilization of Automotive Vehicles Using Active Steering and Adaptive Brake Control Allocation", IEEE Trans. on Control Systems Technology, 2010, vol. 18, pp. 545-558.
[18] Tagesson, K. et al. "Real-time performance of control allocation for actuator coordination in heavy vehicles", Proc. of IEEE Intelligent Vehicles Symposium, 2009, pp. 685-690
[19] Shyrokau, B. et al. "Multi-Task Integrated Vehicle Dynamics Control", Proc. of 13th EAEC European Automotive Congress, 2011, p. 13
[20] Schiebahn, M. et al. "Analysis and Coordination of Multiple Active Systems for Vehicle Dynamics Controls", AVEC'08, 2008.
[21] Lei, Z. et al. "A novel brake control strategy for electric vehicles based on slip trial method", Proc. of IEEE International Conference on Vehicular Electronics and Safety, 2007, pp. 1-6.
[22] Ivanov, V. et al. "Advancement of vehicle dynamics control with monitoring the tire rolling environment", SAE Int. J. of Passenger Cars, 2010, vol. 3, No. 1, pp. 199-216

APPENDIX

The vehicle system is in the affine form:

$$\dot{x} = f(x) + g(x)u$$
$$y = h(x)$$

The states are:

$$x = \begin{bmatrix} \beta & \dot{\psi} \end{bmatrix}^T$$

The nonlinear function is:

$$f(x) = \begin{bmatrix} -\frac{2}{m_a}\left(\frac{(C_{\alpha F}+C_{\alpha R})V_{xa}\beta + (C_{\alpha F}a - C_{\alpha R}b)\dot{\psi} + 0.5m_a V_{xa}^2\dot{\psi}}{V_{xa}^2 - 0.25t_w^2\dot{\psi}^2}\right) - V_{xa}\dot{\psi} \\ -\frac{2}{I_{zz}}\left(\frac{(aC_{\alpha F} - bC_{\alpha R})V_{xa}^2\beta + (a^2C_{\alpha F} + b^2C_{\alpha R})V_{xa}\dot{\psi}}{V_{xa}^2 - 0.25t_w^2\dot{\psi}^2}\right) - f\left(\frac{d\omega_{wi}}{dt}\right) \end{bmatrix}$$

$$f\left(\frac{d\omega_{wi}}{dt}\right) = \frac{t_w}{2I_{zz}}\frac{J_w}{r_w}\left(\frac{d\omega_{w1}}{dt} - \frac{d\omega_{w2}}{dt} + \frac{d\omega_{w3}}{dt} - \frac{d\omega_{w4}}{dt}\right)$$

The control input u is:

$$u = \begin{bmatrix} \delta_F & u_{drive} & u_{brake} \end{bmatrix}^T$$
$$u_{drive} = \begin{bmatrix} M_{fl}^{em} & M_{fr}^{em} & M_{rl}^{em} & M_{rr}^{em} \end{bmatrix}$$
$$u_{brake} = \begin{bmatrix} M_{fl}^{br} & M_{fr}^{br} & M_{rl}^{br} & M_{rr}^{br} \end{bmatrix}$$

The control effectiveness matrix B is calculated as:

$$g(x) \approx B = \begin{bmatrix} B_{steer} & B_{drive} & B_{brake} \end{bmatrix}$$

$$B_{steer} = \begin{bmatrix} \frac{2C_{\alpha F}}{m_a} \\ \frac{2C_{\alpha F}a}{I_{zz}} \end{bmatrix}$$

$$B_{drive} = B_{brake} = \begin{bmatrix} 0 & 0 & 0 & 0 \\ \frac{0.5t_w}{I_{zz}r_w} & -\frac{0.5t_w}{I_{zz}r_w} & \frac{0.5t_w}{I_{zz}r_w} & -\frac{0.5t_w}{I_{zz}r_w} \end{bmatrix}$$